Fabrication techniques for grating-based optical devices

Michael H. Lim,[a] T. E. Murphy, J. Ferrera, J. N. Damask, and Henry I. Smith
Department of Electrical Engineering and Computer Science, MIT, Cambridge, Massachusetts 02139

(Received 1 June 1999; accepted 24 August 1999)

We describe a novel, versatile process for fabricating integrated Bragg-grating devices. Our process addresses many of the critical challenges presented by such devices, including period selection, alignment, spatial coherence, and nanolithography. Using a combination of e-beam, x-ray, optical, and interference lithographies, we have successfully employed this process to construct 244 nm period, quarter-wave-shifted Bragg gratings on top of 1-μm-tall waveguide structures in InP.
© *1999 American Vacuum Society.* [S0734-211X(99)07206-6]

I. INTRODUCTION

The term ''Bragg grating'' refers to an optical device in which a periodic index modulation or structural corrugation reflects light in a narrow wavelength range. The principle of operation is similar to that of a dielectric mirror, in which a periodic sequence of films, of alternating index, is used to achieve high reflectivity over a narrow bandwidth.

Because of their ability to selectively reflect certain wavelengths, Bragg gratings find widespread application in the rapidly growing field of optical telecommunications, especially in wavelength-division multiplexing (WDM). For example, in distributed-feedback lasers, Bragg gratings are used in place of mirrors or facets to provide wavelength-dependent feedback into the lasing medium.[1] Fiber Bragg gratings, in which a periodic index modulation is induced in the core of a photosensitive optical fiber, are now employed for a variety of applications, including dispersion compensation and wavelength add/drop filters.[2]

Relatively sophisticated optical filters can be constructed using Bragg gratings. By changing the pitch and/or modulation depth of the grating across the length of the device, it is possible to tailor the spectral response of the device. Also, by introducing one or more quarter-wave shifts into the grating, it is possible to construct a rich variety of resonator-based filters, from simple Lorentzian bandpass filters to higher-order Butterworth filters.[3,4]

Despite the flexibility afforded by Bragg gratings, their application in integrated-optical devices has been limited to relatively simple components, in part because of the technical challenges in fabricating such structures. In this work, we call attention to these unique challenges and present a process sequence which solves some of the critical problems.

The device we are building to demonstrate these techniques is the channel-dropping filter (CDF), depicted in Fig. 1.[5] The function of the CDF is to drop (or add) one wavelength channel from a multichannel bus. The filtering takes place in the quarter-wave-shifted Bragg gratings located above and below the bus waveguide. Because of the wavelength-selective nature of the Bragg gratings, they act as narrowband resonators, which are only excited by one resonant wavelength channel.

[a]Electronic mail: mhl@nano.mit.edu

II. FABRICATION CHALLENGES

The first challenge presented by the channel-dropping filter depicted in Fig. 1 is that the grating period is ~244 nm, which is beyond the capability of most conventional lithography techniques. Moreover, the presence of an abrupt quarter-wave shift in the grating rules out the use of interference lithography, which otherwise could be used to produce such gratings. In order to fabricate grating filters that include one or more quarter-wave shifts, a more flexible lithography tool, such as electron-beam lithography, must be employed.

A second requirement of the Bragg grating, which is not apparent from Fig. 1, is that the grating must be spatially coherent over its entire length; the Bragg grating is several hundred microns in extent, and therefore must be written by stitching together several e-beam fields. Any appreciable field-stitching errors at the boundaries between these adjacent e-beam fields results in a phase error in the Bragg grating. Stochastic modeling has shown that one must hold the field-stitching error to $\leqslant 5$ nm or else the resulting phase errors cause several deleterious effects in filter function.[6]

For the channel-dropping filter, and more generally for all Bragg-grating-based filters, the operating frequency is determined by the grating period. Therefore, in order to build a narrowband filter for a WDM system, we must maintain precise control of the Bragg-grating period. To illustrate this requirement, consider two consecutive wavelength channels in a dense WDM system, separated in optical frequency by 100 GHz. If our filter is to operate on one of these channels without affecting the other, the period of the Bragg grating must be controlled to within 0.1 nm. In the following section, we describe a technique for reliably measuring and selecting the Bragg period to within 0.1 nm.

Two levels of lithography are required for fabricating the channel-dropping filter shown in Fig. 1: one that defines the waveguide features and a second that defines the fine-pitch gratings on top of the waveguide. Naturally, these two levels of lithography must be aligned relative to one another. In addition to the normal requirements of pattern overlay, the Bragg grating must be oriented such that its features are precisely perpendicular to the direction of the waveguides, i.e., the k-vector of the grating must be precisely aligned to the waveguide axis. Any angular misalignment between the grating and the waveguide axes will cause an effective lengthen-

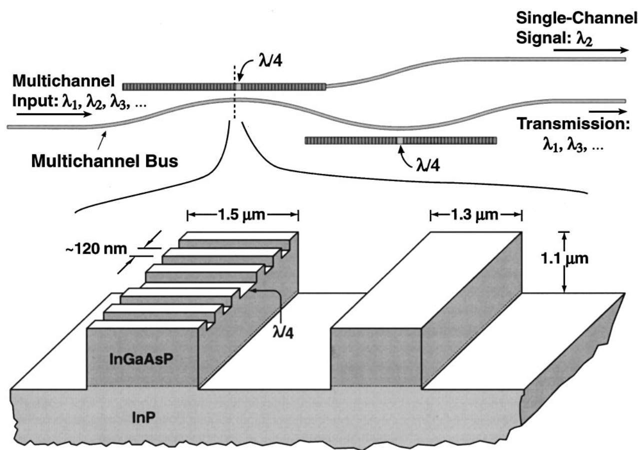

FIG. 1. Schematic of the channel-dropping filter in InP. The quarter-wave-shifted Bragg gratings act as wavelength-selective resonators which separate one wavelength channel from a multiwavelength bus waveguide. The lower portion of this figure illustrates the structure and dimensions of the device. A final layer of InP cladding (not depicted) is deposited over the entire structure to complete the device.

ing of the grating period. Thus, in order to precisely control the operating frequency of the filter, not only must we precisely control the Bragg period as described above, but we must also maintain angular alignment between the grating and the underlying waveguide patterns.

Another challenge presented by the channel-dropping filter is that the fine-period grating structures must be patterned on top of relatively tall waveguide structures. Attempting to spin a coating of high-resolution photoresist onto a substrate with 1.1-μm-tall features invariably results in uneven resist coverage, which leads in turn to unreliable patterning. In order to avoid this topography problem, we have developed a technique that we call the dual-layer-hardmask process (DLHP) which we detail in the following sections.

Finally, once the structure is fabricated, a final layer of InP cladding must be deposited, while maintaining the underlying structure of the device.

III. MASK FABRICATION

In constructing the channel-dropping filter, we use a combination of several lithographies. We use optical-contact photolithography to print the relatively coarse ($\sim 1\ \mu$m) waveguide features, and we use x-ray nanolithography to pattern the fine-period Bragg gratings. The optical photomasks which define the waveguide features were written by a commercial mask shop using a MEBES tool, and the x-ray masks used for the grating features were written with our customized VS2A electron-beam-lithography system.

In generating the x-ray masks required for the channel-dropping filter, we use a technique called spatial-phase-locked e-beam lithography (SPLEBL),[4,7,8] which combines the long-range spatial coherence of interference lithography with the flexibility of electron-beam lithography. In the segmented-grid mode of SPLEBL, interference lithography is first used to generate a coherent ''fiducial'' grating pattern on the x-ray mask. Electron-beam lithography is then used to write the quarter-wave-shifted patterns required by the device. During the e-beam writing, the existing interferometric pattern on the mask is sampled in order to determine the absolute beam position. This technique allows us to generate quarter-wave-shifted gratings that span several e-beam writing fields, yet are free of the interfield stitching errors that would otherwise be present.[4]

Because of the phase locking method used to write the Bragg gratings, the period of the Bragg gratings is proportional to that of the interferometrically generated fiducial gratings on the x-ray mask. Therefore, in order to control the period of the Bragg gratings, it is necessary to control the period of the fiducial gratings to the same relative tolerance, typically to better than one part per thousand. For simplicity of implementation, we have chosen the period of the e-beam grating to be the same as that of the fiducial, although this is not a fundamental requirement.

In interference lithography, the grating period depends upon the wavelength of exposure and the angle between the two beams that form the standing wave, according to

$$p=\frac{\lambda}{2\sin\theta},$$

where λ is the wavelength and θ is the half-angle between the two beams. Although the wavelength is quite accurately controlled, the interference angle θ can only be adjusted to an accuracy of a few milliradians, which is a factor of 5–10 worse than needed. To overcome this difficulty, we measure the period of a test grating using the interferometer-controlled stage of our electron-beam lithography system, and we then fine tune the interference lithography setup to eliminate any period errors. After the test grating is recorded by interference lithography onto a silicon wafer, the sample is electroplated with gold to provide contrast for backscattered electron imaging in the e-beam system. The wafer is mounted on the e-beam stage and the direction of the grating lines with respect to the stage's axes of translation is measured, to eliminate cosine errors. We measure the distance across a large number of periods (250–500) by translating the stage. This distance divided by the number of periods gives the grating period. Figure 2 is a histogram illustrating the high precision achieved with this technique. This gold grating on the Si wafer serves as a reference standard which we use to set up the interference lithography, ensuring that the fiducial grating that we next expose on the x-ray mask has an accurately known period.

When printing gratings onto an x-ray mask using interference lithography, it is not possible to achieve sufficient angular alignment between the standing-wave pattern and a reference direction on the mask. To solve this problem, after the interference lithography is done, we use e-beam lithography to add alignment marks to the x-ray mask which are referenced to the interferometric gratings. After recording the interferometric grating on the x-ray mask, the grating is cleared in selected areas. The mask is then placed in the e-beam lithography tool and the rotation of the grating with respect to the stage axes is measured by recording the (x,y)

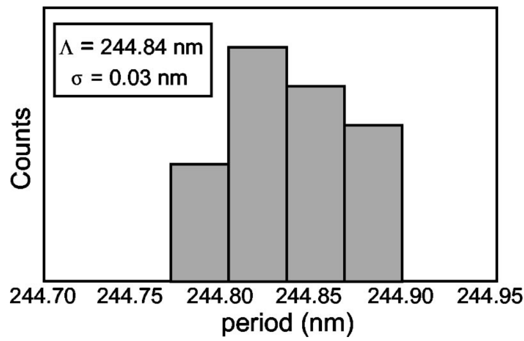

FIG. 2. Histogram demonstrating the precision with which we can measure the period of an interferometrically generated grating. The histogram was obtained by repeatedly measuring the period of the same grating. The accuracy of the measurement is limited by the wavelength of the laser, which is known to 1 part in 10^8, and the cosine error due to misalignment of the stage's interferometer optics and its axes of motion, which we estimate to be less than 1 part in 10^6.

locations of several points along a single grating line, over a distance of approximately 1 cm. Once this calibration has been done, alignment marks—designed to overlay with those from the waveguide photomask—are written in the cleared areas. By means of this technique, we guarantee that the alignment marks placed on the x-ray mask are aligned to the corresponding marks on the waveguide mask to within an angle of 10 μrad. When the x-ray mask is aligned to the waveguide level, the maximum overlay error (measured after exposure) is ~500 nm, corresponding to a maximum total angular misalignment of under 50 μrad.

IV. FABRICATION PROCESS

After the masks are generated, there remains the problem of forming submicron grating patterns over relatively tall surface topography. To address this problem, we have developed a technique that we call the DLHP, which is outlined in Fig. 3. In this process, the Bragg grating patterns are defined first in a thin hard-mask layer on the substrate [Fig. 3(a)]. Before the gratings are etched, however, the waveguide features are patterned in a second hard mask on top of the grating hard mask [Fig. 3(b)]. By patterning both hard masks before the waveguide or grating features are etched into the optical substrate, we ensure that all lithography steps are performed over essentially planar surfaces.

The process begins with an optical substrate of InP with a 1.1-μm-thick layer of InGaAsP quaternary core. Onto the substrate we deposit 50 nm of oxide via e-beam evaporation to serve as the grating hard mask. Then we spin on a 300 nm layer of PMMA and expose it in our x-ray lithography system using the Bragg-grating mask described earlier. We develop the PMMA in a mixture of MIBK:IPA:MEK 21:63:16. After development, we transfer the grating patterns into the oxide using reactive ion etching in a CHF_3 plasma biased to 300 V. Having patterned the grating hard mask, the PMMA is removed.

Because of the method used to generate the x-ray mask, there are auxiliary patterns on the x-ray mask in addition to the quarter-wave-shifted Bragg gratings, i.e., the fiducial gratings. To prevent these patterns from being printed along with the Bragg gratings, we use a second optical lithography step to remove the extraneous features.

Next, we spin on a layer of AZ-5206 photoresist, and expose the waveguide patterns using optical contact photolithography. In this step, we reference to the alignment marks left by the grating mask to ensure angular alignment between the waveguide and Bragg-grating axes. After development, we lift off the waveguide pattern in 200 nm of Ni. Figure 4(a) is a scanning electron micrograph depicting the patterned Ni hard mask layer, with the underlying grating in oxide. We then use the Ni waveguide layer as an etch mask

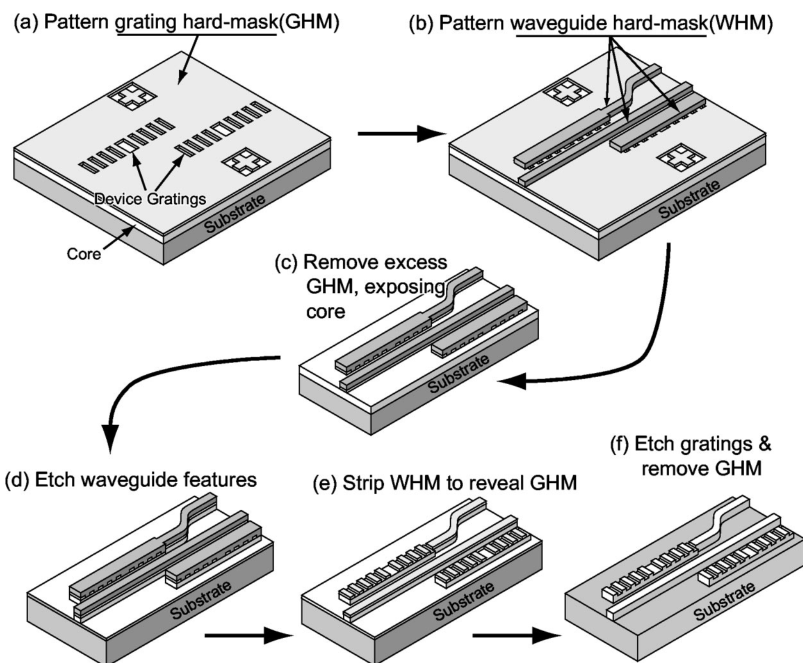

FIG. 3. Outline of the dual-layer-hardmask process (DLHP), which allows us to pattern fine-period gratings over relatively tall waveguide structures. By first patterning two hard-mask layers before forming the structure, we ensure that all lithography steps are performed over essentially planar surfaces.

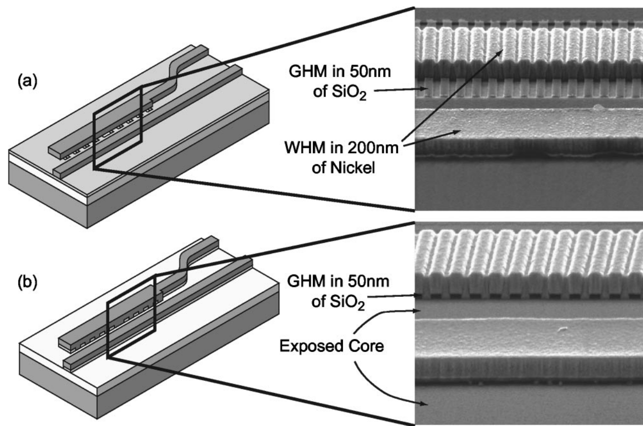

FIG. 4. (a) Scanning electron micrograph showing both the grating hard mask (GHM) and the waveguide hard mask (WHM) used in the process. The waveguide features are patterned with optical photolithography and Ni liftoff, and the underlying gratings are patterned in oxide via x-ray nanolithography and reactive-ion etching. (b) After patterning both hard masks, the excess grating patterns are removed using the waveguide pattern as a mask.

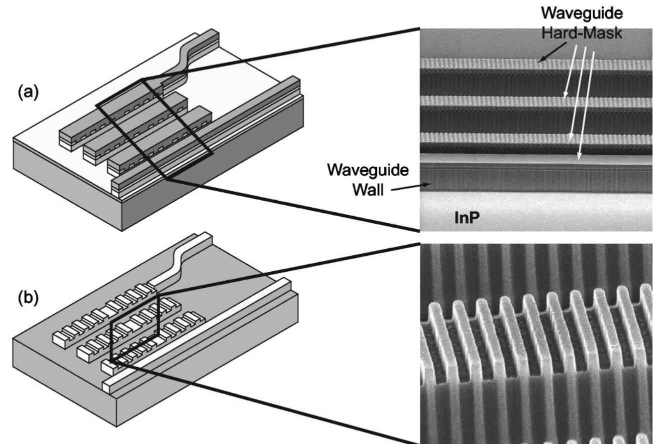

FIG. 5. Scanning electron micrographs showing (a) the etched waveguides; (b) final structure after etching of the gratings and removal of hard masks. (The three parallel gratings shown here are portions of a higher-order filter.)

to clear away any residual grating mask, as shown in Fig. 4(b).

The waveguide features are then etched into the InGaAsP core material, using the Ni layer as hard mask. The InGaAsP is reactive ion etched in a hydrocarbon plasma of $O_2/H_2/CH_4$ at flow rates of 2.5/19/19 sccm. We maintain a DC bias of 300 V and chamber pressure of 4 mTorr. This etch results in straight sidewalls and smooth etch surfaces, as shown in Fig. 5(a). Next, the Ni is removed with a selective wet chemical etch, revealing the underlying oxide grating pattern. Then, the Bragg gratings are etched into the top surface of the waveguide using the oxide hard mask. Finally, the oxide layer is stripped using a solution of buffered HF, completing the process. Figure 5(b) depicts the completed structure after this etch sequence.

The final step in the process is to overgrow a top layer of InP cladding material, thereby forming a buried-channel waveguide structure. Low temperature overgrowth of square-tooth gratings without loss of profile has been demonstrated with gas source molecular beam epitaxy (GSMBE) by Koontz *et al.*[9]

V. CONCLUSIONS

Bragg gratings are important components which offer the potential for a wide range of filtering functions for optical telecommunications. The fabrication challenges presented by Bragg grating devices are quite different from the challenges traditionally confronted by the semiconductor industry. We have developed a process for constructing integrated Bragg gratings which specifically addresses these unique challenges, and demonstrated this process by constructing integrated quarter-wave-shifted Bragg grating devices in InP. Finally, we point out that the techniques described here can easily be applied to other material systems, and other grating geometries.

ACKNOWLEDGMENTS

We wish to acknowledge Mark Mondol who operates the MIT electron-beam-lithography facility, and Charles Joyner (of Lucent Technologies) who generously provided us with InGaAsP/InP materials for this work.

[1]H. Kogelnik and C. V. Shank, J. Appl. Phys. **43**, 2327 (1972).
[2]A. Othonos, Rev. Sci. Instrum. **68**, 4309 (1997).
[3]H. A. Haus and Y. Lai, IEEE J. Quantum Electron. **28**, 205 (1992).
[4]V. V. Wong, J. Ferrera, J. N. Damask, T. E. Murphy, and H. I. Smith, J. Vac. Sci. Technol. B **13**, 2859 (1995).
[5]H. A. Haus and Y. Lai, J. Lightwave Technol. **10**, 57 (1992).
[6]J. Ferrera, J. N. Damask, V. V. Wong, H. I. Smith, and H. A. Haus, Optical Fiber Communication Technical Digest **4**, 139 (1994).
[7]J. Ferrera, V. V. Wong, S. Rishton, V. Boegli, E. H. Anderson, D. P. Kern, and H. I. Smith, J. Vac. Sci. Technol. B **11**, 2342 (1993).
[8]V. V. Wong, J. Ferrera, J. Damask, J. Carter, E. Moon, H. A. Haus, H. I. Smith, and S. Rishton, J. Vac. Sci. Technol. B **12**, 3741 (1994).
[9]E. M. Koontz, M. H. Lim, V. V. Wong, G. S. Petrich, L. A. Kolodziejski, H. I. Smith, K. M. Matney, G. D. U'Ren, and M. S. Goorsky, Appl. Phys. Lett. **71**, 1400 (1997).